Fracture characterization in cancellous bone specimens via surface difference evaluation of 3D registered pre- and post-compression micro-CT scans

M. Prot[a], G. Dubois[a], T. J. Cloete[b], D. Saletti[c] and S. Laporte[a]

[a]LBM/Institut de Biomécanique Humaine Georges Charpark, Arts et Métiers ParisTech, Paris, France; [b]Blast Impact and Survivability Research Unit (BISRU), Department of Mechanical Engineering, University of Cape Town (UCT), Rondebosch, South Africa; [c]Univ. Grenoble Alpes, Grenoble, France

1. Introduction

In recent years, increasingly stringent passenger vehicle safety requirements have led to a renewed interest in the fracture properties of bone. It has been shown that cancellous bone architecture is strongly linked to its overall behavior (Follet et al. 2011; Prot et al. 2015). Micro-fracture mechanisms have been resolved by time-consuming direct microscopy (Prot et al. 2012) or by the use of calcein (Lambers et al. 2014; Hernandez et al. 2014). Furthermore, the application of CT scanners, along with the development of registration algorithms, has allowed separated portions of fractured specimen to be registered to the pre-compression scan so as to quantify the difference between 3D shapes as a mean to characterize the fracture behavior (Tassani & Matsopoulos 2014). However, this method is operator-dependent in the case of multiple fracture zone identification and requires sufficient deformation of the specimen to obtain distinct registration sets. In addition, built-in micro-compression testers, developed by CT scanner manufacturers, are limited to loading at low levels of strain rate, which does not allow measurement over a range that is representative of daily life. The goal of this study was to identify distinct fracture patterns based on micro-CT scans of cancellous bone specimens, loaded over a large range of strain rates, without the need for specimens that have broken into separate pieces.

2. Methods

2.1. Specimens

In total, 126 non-defatted cylindrical cancellous bone specimens (Ø = 10.5 mm, H = 7.5 mm) were extracted from 6 bovine femoral heads in different planes (sagittal, frontal, transversal).

2.2. Architecture acquisition

The pre- and post-compression architecture of the specimens was acquired using a phoenix micro-CT scanner (voxel size 80^3 μm³). The Otsu multi-threshold segmentation was used to automatically separate bone from marrow and background. Multiple specimens were simultaneously positioned in the micro-CT scanner using a custom polystyrene fixture. The thresholds were set to the same levels for both the pre- and post-compression specimens.

2.3. Compression tests

Innovative interrupted compression tests (Prot et al. 2014) were conducted in 3 regimes (Quasi-Static, Intermediate Strain Rate, and Dynamic) covering 8 distinct strain rates: 0.001, 0.01, 0.1, 1, 10, 100, and 600/s. The mechanical properties were extracted from the stress/strain curve.

2.4. Failure pattern analysis

3D bones scans were spatially registered using a rigid transformation algorithm implemented on Avizo. It maximizes the correlation value between the damaged model (post-compression) and the reference (pre-compression) via a linear transformation. This registration scheme based on histograms is suitable as images were identically acquired and binarized. A visualization of the distance between the registered surfaces was used to assess the rupture location.

3. Results and discussion

3.1. Method validation

Three fracture patterns were observed and are presented in Figure 1: asymmetric fracture, progressive compression, and diffuse micro-fractures.
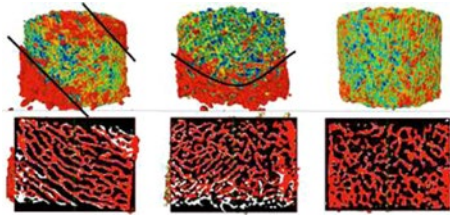

CONTACT M. Prot ✉ marianne.prot@ensam.eu

Figure 1. General fracture morphologies: asymmetric (left), progressive (middle), and diffuse (right).
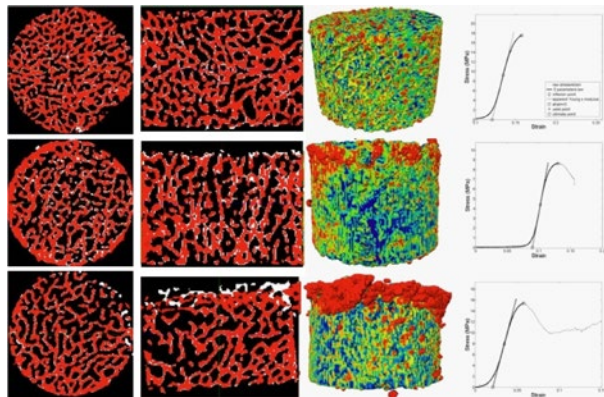

Figure 2. Registered pre- and post-compression scans and the location of the fracture as a function of the deformation.

Ten specimens displayed asymmetric fractures while a further 45 showed progressive compression, both of which were easily identifiable. However, the majority of the specimens presented no noticeable macroscopic fracture but only numerous diffuse micro-fractures throughout the sample. For 11 of these specimens, an alternative registration algorithm, which calculates the distance between the gray values of two images, was used. However, 20% of specimens fell below a minimum deformation threshold and could not be registered with either of the above-mentioned methods.

At present, the method of visualizing the inter-surface distances is primarily qualitative for diffuse fracture while the nominal angle of the crack with asymmetric fractures can be determined and interpreted with respect to the micro-architecture. The full complexity of the fracture geometry could not be assessed. Several alternative methods based on features of the image correlation process, such as the distances between nodes of a skeletonize 3D image, or between beams, or by meshing the surface, are under consideration to overcome these limitations.

3.2. Deformation and fracture

Despite the current limitations, a registered image allows the fracture behavior to be related to the deformation of a specimen. Typical results are shown in Figure 2, where progressive rupture is visible depending on the deformation of the specimen. In the first row of images, the stress/strain curve indicates that the linear response limit was exceeded, but the corresponding 0.2 mm deformation is not evident on rigid readjustments of the registered image. In other words, the specimen displayed viscoelastic recovery. The results shown in the other two rows indicate that this recovery disappears with increase of fracture damage. The aim of ongoing work is to quantify this relaxation behavior as a function of the strain rate and the marrow contribution.

4. Conclusions

This study highlights the potential use of micro-CT scans to investigate the initiation and development of fracture in cancellous bone specimens subjected to different rates of loading in compression. Ongoing work will focus on quantifying the damage so as to correlate it with the micro-structural organization.

References

Follet H, Viguet-Carrin S, Burt-Pichat B, Dépalle B, Bala Y, Gineyts E, Munoz F, Arlot M, Boivin G, Chapurlat, Delmas PD. 2011. Effects of preexisting microdamage, collagen cross-links, degree of mineralization, age, and architecture on compressive mechanical properties of elderly human vertebral trabecular bone. J Orthop Res. 29:481–488.

Hernandez CJ, Lambers FM, Widjaja J, Chapa C, Rimnac CM. 2014. Quantitative relationships between microdamage and cancellous bone strength and stiffness. Bone. 66:205–213.

Lambers FM, Bouman AR, Tkachenko EV, Keaveny TM, Hernandez CJ. 2014. The effects of tensile-compressive loading mode and microarchitecture on microdamage in human vertebral cancellous bone. J Biomech. 47:3605–3612.

Prot M, Cloete TJ, Pattofatto S. 2012. Dynamic compression and recovery of cancellous bone for microstructural investigation. In EPJ Web Conf. Vol. 26, p. 03003.

Prot M, Cloete TJ, Saletti D, Laporte S. 2014. Intermediate strain rate behaviour of cancellous bone: from the lower to the higher strain rate. Comput Methods Biomech Biomed Eng. 17(Suppl 1):50–51.

Prot M, Saletti D, Pattofatto S, Bousson V, Laporte S. 2015. Links between mechanical behavior of cancellous bone and its microstructural properties under dynamic loading. J Biomech. 48:498–503.

Tassani S, Matsopoulos GK. 2014. The micro-structure of bone trabecular fracture: an inter-site study. Bone. 60:78–86.